(s), 885 (s), 850 (m), 815 (s), 750 (s), 710 (s), 610 cm^{-1} (m).

Anal. Calcd for $C_{18}H_{19}N$: C, 86.70; H, 7.68; N, 5.62. Found: C, 86.57; H, 7.68; N, 5.60.

Anthracene from 12. To a magnetically stirred solution of **12** (0.1 g, 0.4 mmol) in CH_2Cl_2 (10 mL) at 25 °C was added *m*-CPBA (0.06 g, 0.4 mmol). The resulting aqua solution was stirred at 25 °C for 1 h and then preadsorbed onto activity III basic Al_2O_3. Chromatography over activity III basic Al_2O_3 (hexane) gave 0.06 g (86%) of anthracene: mp 217–218 °C, identical (IR, TLC, UV, mmp 217–218 °C) to a commercial sample.

13-Methyl-5,12-dihydronaphthacen-5,12-imine (15). This reaction was carried out as described for **10**, employing the following materials: **9** (1.0 g, 3.5 mmol), 2-methylisoindole (**13**;[12a] 1.5 g, 0.01 mol), THF (25 mL), and phenyllithium (1.80 M in cyclohexane; 2.0 mL, 3.5 mmol). The usual workup and chromatography gave 0.47 g (52%) of **15** as a tan solid. Recrystallization from hexane gave the analytical sample: mp 168–169 °C; ^1H NMR ($CDCl_3$) δ 2.25 (s, 3 H), 5.00 (s, 2 H), 7.1 (m, 6 H), 7.65 (s, 4 H); ^{13}C NMR ($CDCl_3$) δ 36.4, 72.3, 120.6, 121.6, 125.6, 125.8, 127.7, 132.3, 144.0, 147.1; IR (KBr) 2980 (w), 2960 (w), 1450 (w), 1270 (w), 940 (m), 885 (m), 780 (s), 740 (s), 700 (s), 695 (s), 640 cm^{-1} (m).

Anal. Calcd for $C_{19}H_{15}N$: C, 88.68; H, 5.88; N, 5.44. Found: C, 88.50; H, 5.91; N, 5.45.

13-Methyl-1,2,3,4-tetrafluoro-5,12-dihydronaphthacen-5,12-imine (16). This reaction was carried out as described for **10**, employing the following materials: **9** (1.0 g, 3.5 mmol), 2-methyl-4,5,6,7-tetrafluoroisoindole; (**14**;[12b] 1.5 g, 7.4 mmol), THF (25 mL), and phenyllithium (1.80 M in cyclohexane; 2.0 mL, 3.5 mmol). The usual workup and chromatography gave 0.78 g (68%) of **16** as white flakes. Recrystallization from hexane gave the analytical sample: mp 186–187 °C; ^1H NMR ($CDCl_3$) δ 2.30 (s, 3 H), 5.35 (s, 2 H), 7.5 (m, 2 H), 7.75 (s, 4 H); ^{13}C NMR ($CDCl_3$) δ 36.2, 69.4, 120.9, 126.3, 127.9, 132.3, 141.3; IR (KBr) 2960 (w), 1500 (s), 1280 (s), 1205 (m), 1190 (m), 1100 (m), 1050 (s), 955 (m), 760 (s), 745 cm^{-1} (m).

Anal. Calcd for $C_{19}H_{11}NF_4$: C, 69.30; H, 3.37; N, 4.25. Found: C, 69.39; H, 3.55; N, 4.14.

Naphthacene (1). To a magnetically stirred solution of **15** (0.08 g, 0.3 mmol) in MeCN (25 mL) at 25 °C was added *m*-CPBA (0.05 g, 0.3 mmol). The resulting solution was refluxed for 2 h, during which time a green fluorescence developed and an orange solid appeared. The mixture was cooled and filtered to afford 0.06 g (85%) of **1** as orange flakes: mp 356–357 °C, identical (IR, TLC, UV, mmp 356–357 °C) to a commercial sample.

1,2,3,4-Tetrafluoronaphthacene (17). To a magnetically stirred solution of **16** (0.03 g, 0.09 mmol) in $CHCl_3$ (10 mL) at 25 °C under N_2 was added 50% aqueous NaOH (2 drops) and benzyltriethylammonium chloride (5 mg). The resulting mildly exothermic reaction was stirred at 25 °C overnight, during which time the solution became orange with a green fluorescence. The solution was partitioned between 3 N HCl (20 mL) and $CHCl_3$ (50 mL). The organic layer was washed with H_2O, dried (K_2CO_3), and evaporated in vacuo to afford **17** as an orange solid. Recrystallization from benzene–hexane afforded 0.025 g (92%) of **17** as orange needles: mp 263–264 °C; IR (KBr) 1590 (m), 1490 (s), 1385 (m), 1100 (m), 1000 (m), 990 (m), 890 (m), 810 (m), 790 (m), 730 cm^{-1} (s); UV (benzene) λ_{max} 473, 443, 416, 392, 295, 278 nm.

Anal. Calcd for $C_{18}H_8F_4$: C, 72.01; H, 2.69. Found: C, 71.84; H, 2.82.

Acknowledgment. This investigation was supported by PHS Grant CA-24422, awarded by the National Cancer Institute, DHEW, and in part by Grant CH-200 from the American Cancer Society and by Merck Sharp and Dohme Research Laboratories.

Registry No. 1, 92-24-0; 3, 19873-31-5; 7, 80789-65-7; 8, 6710-98-1; 9, 13214-70-5; 10, 22187-13-9; 11, 85894-21-9; 12, 85894-22-0; 13, 33804-84-1; 14, 38053-09-7; 15, 85894-23-1; 16, 85908-81-2; 17, 29525-05-1; *N-tert*-butylpyrrole, 24764-40-7; furan, 110-00-9; anthracene, 120-12-7.

Acidolysis of Ozonides. An ab Initio Study

Masahiro Miura,[1a] Shigeru Nagase,*[1b] Masatomo Nojima,*[1a] and Shigekazu Kusabayashi[1a]

Department of Applied Chemistry, Faculty of Engineering, Osaka University, Suita, Osaka 565, Japan, and Department of Chemistry, Faculty of Education, Yokohama National University, Hodogaya-ku, Yokohama 240, Japan

Received September 21, 1982

As the model species of the intermediates which may participate in the acidolysis of ozonides, seven species **14–20** have been investigated with the ab initio SCF–MO method at the split-valence 4-31G level. On the basis of both the relative stabilities and the charge distributions of these species, we have attempted to provide insight into the apparently complicated experimental observations.

Acidolysis of ozonides (1,2,4-trioxolanes) has been found to proceed by several pathways, depending on the structure of ozonides and reaction conditions.[2] The following examples discovered by us[3-6] illustrate this situation. (a) The reaction of triphenylethylene ozonide (**1**) in methylene chloride gave equimolar proportions of benzophenone (**2**) and phenyl formate (**3**) (eq 1),[3] while in methanol its reaction afforded methyl benzoate (**4**) (via α-methoxybenzyl hydroperoxide) along with **2** (eq 2).[4] The former reaction seems to proceed via heterolytic cleavage of the C–O bond of the ether bridge. Probably C–O bond fission of the

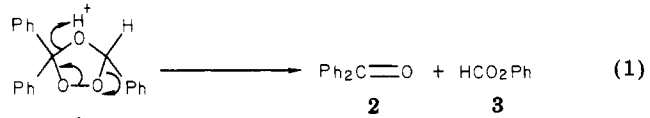

1 2 3 (1)

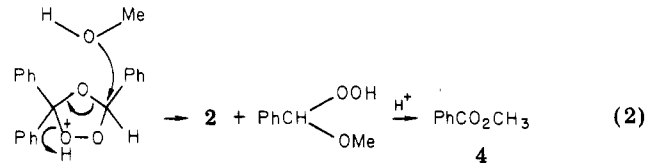

4 (2)

(1) (a) Osaka University. (b) Yokohama National University.
(2) Bailey, P. S. "Ozonation in Organic Chemistry"; Academic Press: New York, 1978; Vol. 1; *Ibid.*, 1982, Vol. 2.
(3) Miura, M.; Nojima, M. *J. Am. Chem. Soc.* **1980**, *102*, 288.
(4) Miura, M.; Nojima, M.; Kusabayashi, S. *J. Chem. Soc., Perkin Trans. 1* **1980**, 2909.
(5) Miura, M.; Nojima, M.; Kusabayashi, S.; Nagase, S. *J. Am. Chem. Soc.* **1981**, *103*, 1789.
(6) Miura, M.; Ikegami, A.; Nojima, M.; Kusabayashi, S.; McCullough, K. J.; Nagase, S. *J. Am. Chem. Soc.* **1983**, *105*, 2414.

0022-3263/83/1948-2366$01.50/0

Chart I

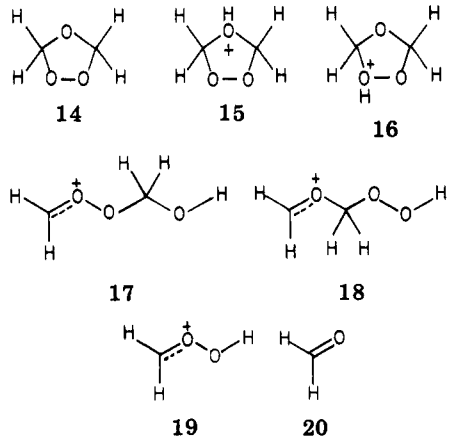

peroxide bridge is a key step for the latter reaction. (c) When a mixture of 1-phenylcyclopentene ozonide (5) and stilbene ozonide (6) was treated with catalytic amounts of chlorosulfuric acid in methylene chloride, 1,4-diphenyl-2,3,5,6,11-pentaoxabicyclo[5.3.1]undecane (8) was obtained. By contrast, the reaction of a mixture of 5 and 1-methylcyclopentene ozonide (7) afforded the pentaoxabicycloundecane 9 (eq 3).[5] We have tentatively suggested

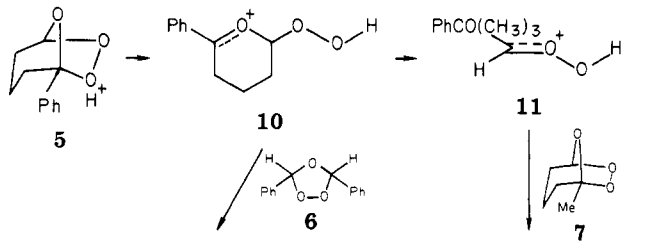

(3)

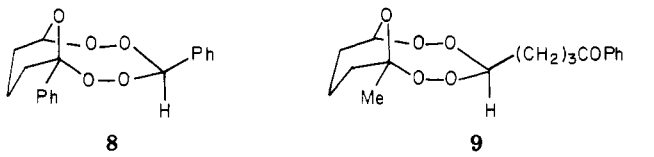

(4)

that the carboxonium ion 10 is a key intermediate in the former reaction, while the protonated carbonyl oxide 11, formed from 10 by electron migration, would participate in the formation of 9. (d) From exo ozonide 12 or endo isomer 13 was obtained an equilibrium mixture of 12 and 13 (the 12/13 ratio of 7:3) (eq 4).[6] This result would come from the cleavage of two C–O bonds of the ozonides.

In an attempt to interpret these apparently complicated but interesting behaviors of ozonides under acidic conditions and also to obtain a criterion for further study, model calculations of the intermediates must be most profitable. For these purposes, seven species, 14–20 (Chart I), were considered and investigated with the ab initio SCF–MO method at the split-valence 4-31G level.

Results and Discussion

All ab initio calculations with the split-valence 4-31G basis set[7] were carried out within the restricted Hartree–Fock SCF approximation by using an IMS version of the GAUSSIAN 80 series of programs.[8] The molecular geometries of the model species 14–20 were fully optimized with analytical energy gradients and a procedure developed by Schlegel.[8c] In Table I are given the 4-31G calculated total energies of these species. The energies relative to ozonide 14 are summarized in Figure 1.

Table I. Energies of the Modela Species

species	energy, hartrees	species	energy, hartrees
14	−302.06999	18	−302.38010
15	−302.36283	19	−188.63064
16	−302.35208	20	−113.69262
17	−302.36143	H^+	0.0

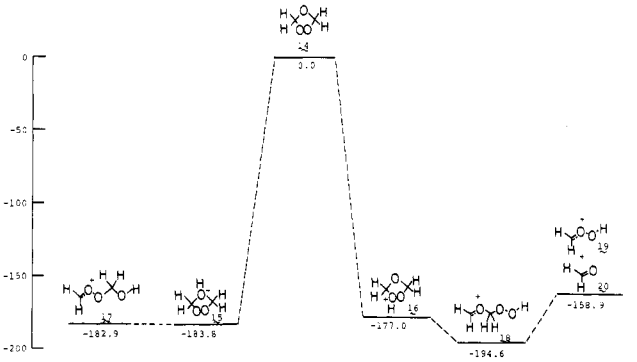

Figure 1. Relative energies of (kcal/mol) of the model species; ozonide 14 is taken as the standard.

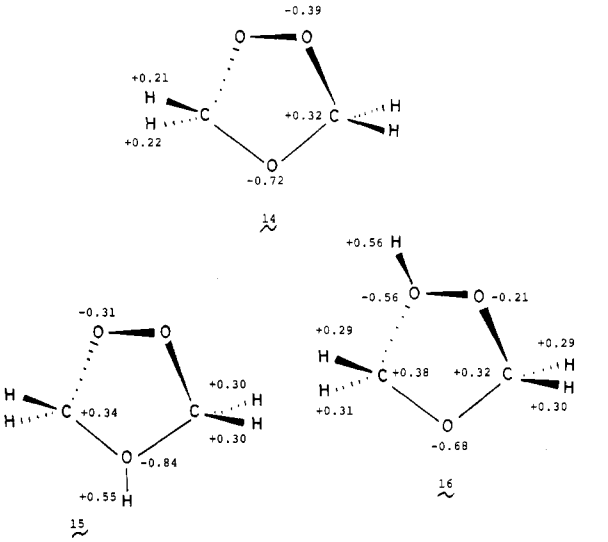

Figure 2. Charge densities of 14–16.

Protonation of Ozonide. Both the ether oxygen and the peroxidic oxygen of ethylene ozonide (14) are possible sites to be protonated (eq 5). As the charge distribution

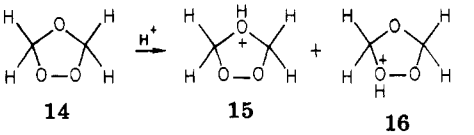

(5)

of 14 suggests (Figure 2), ether oxygen is the more basic site. In accordance with this, the ozonide protonated at

(7) Ditchfield, R.; Hehre, W. J.; Pople, J. A. *J. Chem. Phys.* **1971**, *54*, 724.

(8) (a) Binkley, J. S.; Whiteside, R. A.; Krishman, R.; Seeger, R.; De Frees, D. J.; Schlegel, H. B.; Topiol, S.; Kahn, L. R.; Pople, J. A. *QCPE* **1981**, *10*, 406. (b) An IMS version of the GAUSSIAN 80 program was coded by K. Hori, Y. Teramae, and A. Yamashita at the Computer Center of IMS. (c) Schlegel, H. B. *J. Comput. Chem.* **1982**, *3*, 214.

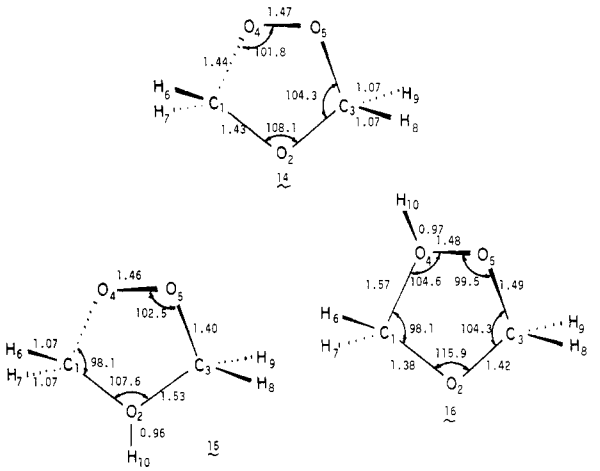

Figure 3. Geometries of **14–16**; distances are in angstroms and angles in degrees.

the ether oxygen, **15**, is 7 kcal/mol more stable than the ozonide protonated at the peroxidic oxygen **16**. Protonation is therefore expected to occur at the ether oxygen preferably. The difference in energy between **15** and (**14** + proton) is as large as 184 kcal/mol, the former being much more stable. This fact demonstrates that the contribution of **15** would be significant in the presence of an acid catalyst in nonpolar solvents.[9]

Cleavage of the C–O Bond of the Ether Bridge. As the geometrical difference between **14** and **15** indicates (Figure 3), protonation at the ether oxygen is accompanied by lengthening the C–O bond of the ether bridge (the distances and angles are in angstroms and degrees; the numbering systems adopted for this study are shown in the figures of the optimized geometries in each case). The most stable conformation of **15** is an oxygen–oxygen half-chair, in which the hydrogen at the 2-position (H-10) is placed on a plane built by the atoms C(1), O(2), and C(3). It is noted that ozonide **14** also adopts an oxygen–oxygen half-chair conformation,[10] this conclusion being in harmony with that from microwave spectral studies.[11] The reaction of **15** would begin with cleavage of the C–O bond of the ether bridge (eq 6). The carboxonium ion **17**, thus formed,

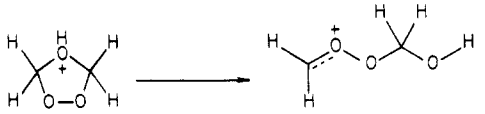

15 **17** (6)

is 1 kcal/mol less stable than **15**. The optimized geometry of **17** indicates that the atoms H(6), H(7), C(1), O(4), and O(5) are placed essentially on the same plane, while the carbon at 3-position is slightly above the plane (Figure 4).

The most probable mode of decay of **17** would involve electronic reorganization, followed by hydride migration and the subsequent deprotonation to yield equimolar proportions of formaldehyde and formic acid (see eq 1). In order for this process via **15** to contribute in a significant amount, two conditions, i.e., easy cleavage of the C–O bond and possesion of a substituent with a large migrating ability to the oxygen at the 5-position, must be satisfied. Tet-

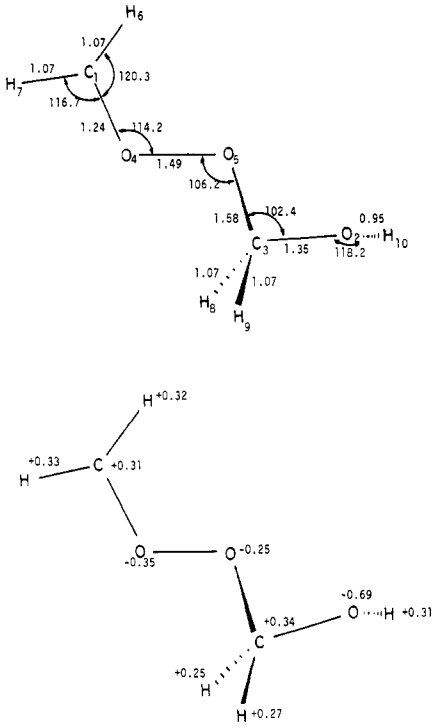

Figure 4. Geometry and charge density of **17**; distances are in angstroms and angles in degrees.

raphenylethylene ozonide satisfies these conditions, affording a mixture of benzophenone and phenyl benzoate in a molar ratio of 1:1.[3] By contrast, 1,1-diphenylheptene 1-ozonide (**21**) gave a mixture of 3,6-dipentyl-1,2,4,5-tetroxane (**22**) and **2** in yields of 41% and 82%, respectively (eq 7).[3] A mechanism involving C–O bond fission of the

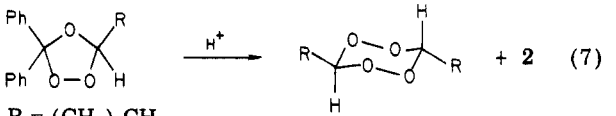

21, R = $(CH_2)_4CH_3$ **22**, R = $(CH_2)_4CH_3$ (7)

peroxide bridge in the first step of the reaction explains well the formation of tetroxane **22** (the detail will be discussed later). It should be noted that if the reaction of **21** begins with cleavage of the C–O bond of the ether bridge, the hydrogen having a relatively smaller migrating ability must migrate toward the oxygen at the 5-position to afford hexanoic acid along with benzophenone (**2**).

Cleavage of the C–O Bond of the Peroxide Bridge. Cleavage of the C–O bond of a protonated ozonide **16** leads to the formation of a carboxonium ion **18** (eq 8); as is

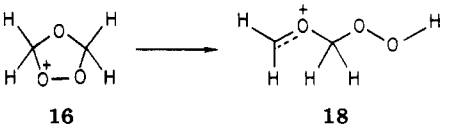

16 **18** (8)

obvious from the comparison in geometry of **14** and **16**, upon protonation at the peroxidic oxygen both the C(1)–O(4) bond length and the C(1)–O(2)–C(3) angle increase to a significant extent. It is notable that the carboxonium ion **18** is calculated to be 18 kcal/mol more stable than the protonated ozonide **16**. Therefore, protonation of ozonide **14** at the peroxidic oxygen, if it occurs, would be followed by a smooth cleavage of the C–O bond to afford **18**. Consistent with this, treatment of phenylcyclopentene ozonide (**5**) with equimolar amounts of $SbCl_5$ affords a zwitter ion **23** (eq 9). The geometry of **18** (Figure 5) indicates that the atoms H(6), H(7), C(1), O(2), C(3),

(9) Since the relative stabilities of the species **14–20** can be influenced by solvation, considerable care should be exercised especially in polar solvents. Caution may also need to be taken for correlation effects (not considered in the present calculations).

(10) (a) Cremer, D. *J. Am. Chem. Soc.* **1981**, *103*, 3627. (b) Hiberty, P. C.; Leforestier, C. *Ibid.* **1978**, *100*, 2012. (c) Harding, L. B.; Goddard, W. A., III. *Ibid.* **1978**, *100*, 7180.

(11) Mazur, U.; Kuczkowski, R. L. *J. Mol. Spectrosc.* **1980**, *65*, 84.

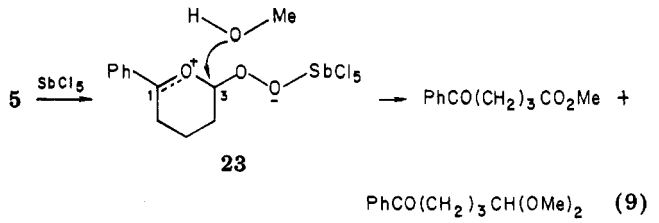

23

$$PhCO(CH_2)_3CH(OMe)_2 \quad (9)$$

and O(5) are placed almost on a same plane, while the oxygen at the 4-position is placed upper to the plane. The C(1)–O(2) bond is as short as 1.24 Å, suggesting that this bond has a double bond character to a significant extent.

As the charge distribution shows (Figure 5), the carboxonium ion **18** behaves as an ambident electrophile. Stilbene ozonide (**6**), as a powerful nucleophile, is prone to attack the C(1) of the zwitter ion **23** (see eq 3),[5] while methanol, a poor nucleophile, attacks the C(3) of **23** (eq 9).[5,12] In connection with this, most of the experimental results we have obtained seem to suggest that the processes leading to final products via carboxonium ion **18** are more advantageous than the ones via carboxonium ion **17**, i.e.: (a) the reaction of triphenylethylene ozonide (**1**) with methanol proceeds via α-methoxybenzyl hydroperoxide (eq 2), (b) treatment of **5** with $SbCl_5$ yields the corresponding zwitter ion **23** (eq 9), and (c) the reaction of *exo*-ozonide **12** clearly indicates the participation of the corresponding carboxonium ion **24** (eq 10 and Scheme I).[6] If consider-

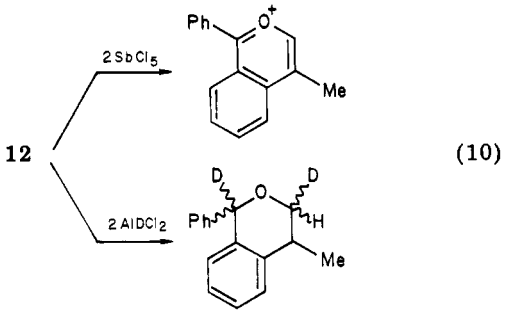

(10)

ation is given to the facts that (a) protonation of **14** occurs predominantly at the ether oxygen to yield **15** and (b) the difference in energy between **15** and carboxonium ion **17** is as small as 1 kcal/mol, a question may arise as to why the process via the carboxonium ion **17** does not contribute to a significant extent. Although we are, at this stage, not able to provide a clear account, it would be worth noting that among the possible intermediates participating in the acidolysis of ozonides, carboxonium ion **18** is calculated to be the most stable; under the reaction conditions we have investigated, therefore, the intermediate **18** would be forced to be produced predominantly for some unexplained reason.[13]

Protonated Carbonyl Oxide 19 from Carboxonium Ion 18. A most interesting problem in the acidolysis of ozonide **14** is to see if a mixture of protonated carbonyl oxide **19** and formaldehyde (**20**) is formed from carboxonium ion **18** by electron migration (eq 11). As Figure 6

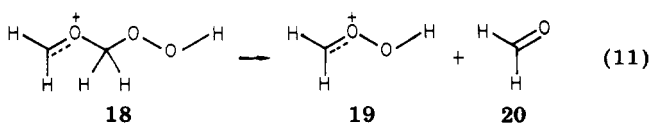

18 19 20 (11)

(12) (a) Miura, M.; Ikegami, A.; Nojima, M.; Kusabayashi, S. *J. Chem. Soc., Chem. Commun.* **1980**, 1279. (b) Miura, M.; Yoshida, M.; Nojima, M.; Kusabayashi, S. *Ibid.* **1982**, 397.

(13) Although a refree suggests that a knowledge of transition states connecting **15** and **17** or **16** or **18** is helpful, at this time it is too time consuming for us to determine them with the 4-31G basis set.

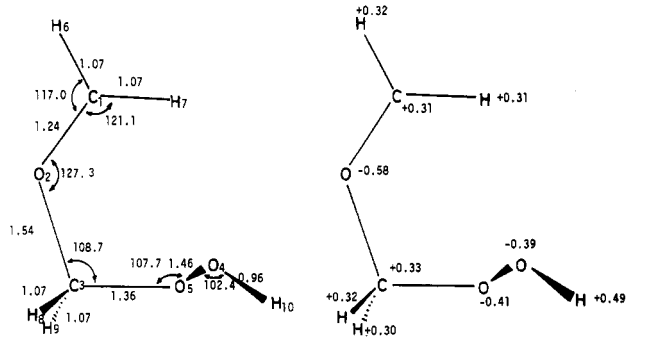

Figure 5. Geometry and charge density of **18**; distances are in angstroms and angles in degrees.

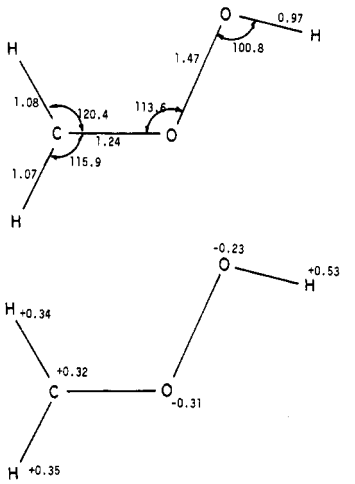

Figure 6. Geometry and charge density of **19**; distances are in angstroms and angles in degrees.

Scheme I

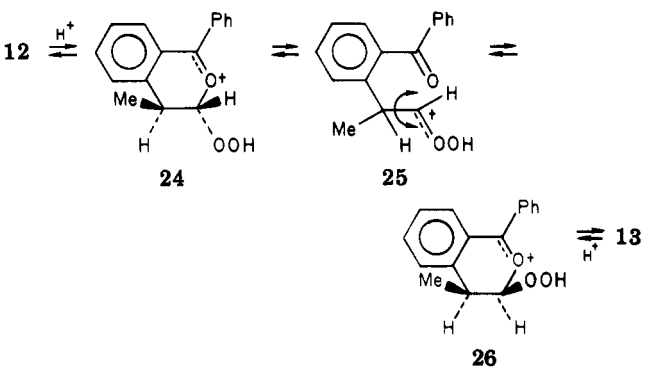

shows, **19** has a planar structure, with the C–O bond being only 1.24 Å. Figure 1 shows that carboxonium ion **18** is 36 kcal/mol more stable than protonated carbonyl oxide **19** plus formaldehyde (**20**). The calculated mode of decomposition of carboxonium ion **18** leading to **19** to **20** is illustrated in Figure 7; it is found that there is no barrier to the formation of **19** plus **20**.

Although the present calculations indicate that the process leading to **19** is energetically unfavorable, the interconversion between *exo*-ozonide **12** and the endo isomer **13** (eq 4) seems to be best rationalized by a mechanism involving the participation of protonated carbonyl oxide **25** (Scheme I). If consideration is given to the fact that in the reaction of **12** the carboxonium ion **24** is a key intermediate leading to products (eq 10), the same carboxonium ion **24** is most likely to be produced in the first step of this rearrangement of **12** to **13**. Electron migration leads **24** to the protonated carbonyl oxide **25**. Subsequent C–C

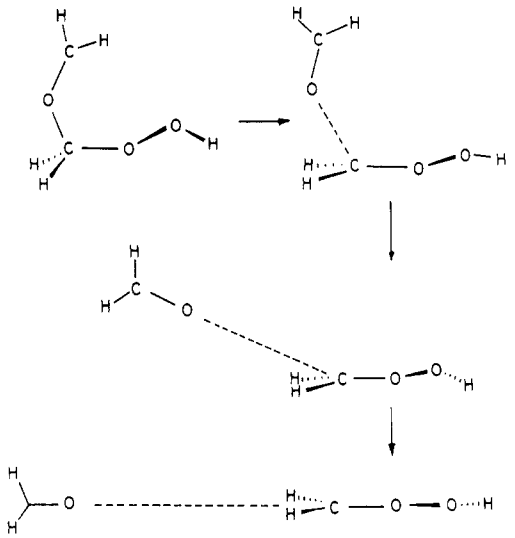

Figure 7. Mode of decomposition of **18** leading to **19** plus **20**.

bond rotation, followed by rebonding of the carbonyl oxygen and the positive carbon, would yield the two carboxonium ions **24** and **26**, which in turn would give the *exo*-ozonide **12** and the endo isomer **13**, respectively. As the following fact suggests, however, protonated carbonyl oxide **25** does not seem to be a stable intermediate. When **12** was treated with bis(α-hydroxy-*p*-methylbenzyl) peroxide (**27**) in the presence of 0.1 molar equiv of $ClSO_3H$ in acetic acid at 20 °C for 4 h, a mixture of an *exo*-peroxide, **28**, and the endo isomer **29** was obtained in a yield of 19% (the **28**/**29** ratio = ca. 1:1). In addition, the recovered ozonide (24%) was a mixture of 70% *exo*-**12** and 30% *endo*-**13** ozonides (Scheme II). The reaction of **13** under the same conditions gave exactly the same result. This fact suggests that equilibration of two isomeric ozonides **12** and **13** is faster than capture of the carboxonium ions **24** and **26** by the nucleophile **27**.[14] In other words, if the carboxonium ion **24** is formed, equilibration of **24** and **26** via the protonated carbonyl oxide **25** occurs immediately, which results in the reformation of a mixture of **12** and **13**. If the protonated carbonyl oxide **25** were a stable intermediate, the tetroxane **30** should have been formed in a considerable amount; we failed, however, to isolate it. Thus, protonated carbonyl oxide **25**, is formed, would be at most considered as an unstable intermediate. This conclusion leads us to deduce that the tetroxane **22** obtained from the acid-catalyzed decomposition of 1,1-diphenylheptene 1-ozonide (**21**) (eq 7) is formed by a mechanism involving attack by the ozonide **21** on the C-3 of the carboxonium ion **31** (Scheme III).

(14) Treatment of **12** with 0.1 equiv of $ClSO_3H$ in methanol at 20 °C for 4 h, however, resulted in the recovery of only the exo ozonide (21%) along with **31** (37%) and **32** (28%) (eq 12).[6] This result may be interpreted as capture of the carboxonium ion **24** by methanol being significantly faster than the isomerization of **24** to **26** via **25**.

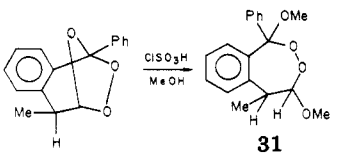

31

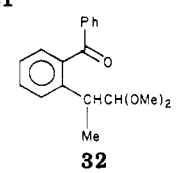

(12)

32

Scheme II[a]

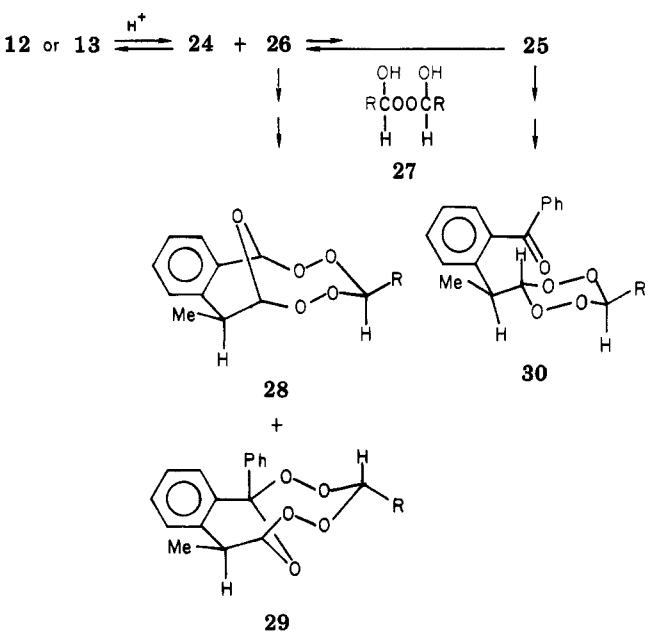

[a] R = 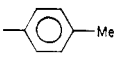

Scheme III[a]

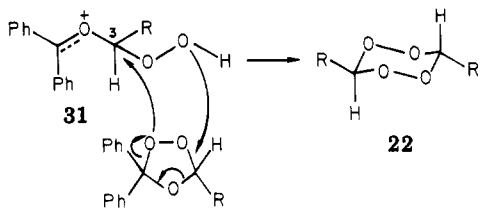

[a] R = $(CH_2)_3CH_3$

Conclusion

As the experimental results suggest, the substituents of the ozonide, nucleophiles, and solvents affect remarkably the reaction pathways in the acidolysis of ozonides. However, the behavior is mostly consistent with that expected from the MO calculations of the model species **14**–**20**. Important information obtained by these calculations is as follows. (a) Protonation of ozonide occurs mainly at the ether oxygen. (b) The carboxonium ion **17**, formed from **15** by electron migration, is 1 kcal/mol less stable than **15**. (c) The carboxonium ion **18** is 18 kcal/mol more stable than **16**. Thus, protonation of **14** at the peroxidic oxygen, if it occurs, would be followed by smooth cleavage of the C–O bond of the peroxide bridge to afford **18**. (d) Both the 1-position and the 3-position of **18** have similar charge densities, suggesting that carboxonium ion **18** behaves as an ambident electrophile. (d) Protonated carbonyl oxide **19** plus formaldehyde (**20**) is 37 kcal/mol less stable than **18**, suggesting that electronic reorganization of **18** leading to **19** plus **20** is not a favorable process.

Acknowledgment. All computations have been carried out at the Computer Center of the Institute for Molecular Science by using the computer center library program GAUSS0 (WF10-025).[8]

Registry No. **14**, 289-14-5; **15**, 85894-31-1; **17**, 85894-32-2; **18**, 85894-33-3; **19**, 85894-34-4; **20**, 50-00-0.

Supplementary Material Available: Table II, the geometries of species **14**–**18** (3 pages). Ordering information is given on any current masthead page.